A&A, 707, C2 (2026)
https://doi.org/10.1051/0004-6361/202659393e

Astronomy & Astrophysics

Multi-wavelength observations of the luminous fast blue optical transient AT 2023fhn

Up to ~200 days post-explosion *(Corrigendum)*

A. A. Chrimes[1,2,⋆,⋆⋆], D. L. Coppejans[3], P. G. Jonker[2], A. J. Levan[2,3], P. J. Groot[2,4,5], A. Mummery[6], and E. R. Stanway[3]

[1] European Space Agency (ESA), European Space Research and Technology Centre (ESTEC), Keplerlaan 1, 2201 AZ Noordwijk, The Netherlands
[2] Department of Astrophysics/IMAPP, Radboud University, PO Box 9010, 6500 GL Nijmegen, The Netherlands
[3] Department of Physics, University of Warwick, Gibbet Hill Road, CV4 7AL Coventry, United Kingdom
[4] Inter-University Institute for Data Intensive Astronomy, Department of Astronomy, University of Cape Town, Private Bag X3, Rondebosch 7701, South Africa
[5] South African Astronomical Observatory, P.O. Box 9, 7935 Observatory, South Africa
[6] School of Natural Sciences, Institute for Advanced Study, 1 Einstein Drive, Princeton, NJ 08540, USA

A&A, 691, A329 (2024), https://doi.org/10.1051/0004-6361/202451172

Key words. errata, addenda – stars: black holes – circumstellar matter – supernovae: general – stars: winds, outflows – supernovae: individual: AT2023fhn

1. Revised X-ray luminosities

In the published paper, we adopted a photon index (Γ) of 2 when calculating *Chandra* X-ray fluxes of the luminous fast blue optical transient (LFBOT) AT2023fhn. Based on these results, we claimed that AT2023fhn was under-luminous in X-rays with respect to other LFBOTs, including the proto-typical AT2018cow (e.g. Kuin et al. 2019). When the measurements are made without fixing Γ, we obtain higher fluxes. For each epoch, we performed spectral fitting with SHERPA (Siemiginowska et al. 2024) by first modelling the background as a power law, freezing these parameters (i.e. the normalisation and photon index, $\Gamma_{\rm bkg}$) and then modelling the spectrum at the source position as the sum of the predetermined (scaled) background and a source power law. We find that while Γ is poorly constrained (in epoch 1 we find $\Gamma_{\rm bkg} = 0.9 \pm 0.4$ and $\Gamma = 0.7^{+0.4}_{-0.5}$), this nevertheless indicates that the spectra are harder than previously assumed. The new fluxes in the 0.5–10 keV range, corrected for an X-ray absorption column density of $N_{\rm H} = 2.6 \times 10^{20}$ cm^{-2}, are provided in Table 1. The corresponding luminosities (for a redshift $z = 0.24$) are shown in Fig. 1 (see also Nayana et al. 2025 and Sevilla et al. 2026, who also present new, higher fluxes), and the updated X-ray/UV ratios in Fig. 2. Given the increased luminosities, we no longer claim that AT2023fhn was sub-luminous in X-rays with respect to AT2018cow in particular. However, we note that there is still significant variation in the population (see Fig. 1).

2. D_L versus D_θ in synchrotron blast-wave modelling

In the original paper we calculated the circumstellar properties of AT2023fhn based on radio observations and synchrotron blast-wave modelling following Chevalier (1998) and DeMarchi et al. (2022). These properties included the emission radius (R_p), Lorentz factor of the outflow ($\Gamma\beta$), wind density parameter ($\dot{M}/V_w$), electron density (n_e), internal magnetic field (B), and internal energy of the shock (U). In these calculations, we erroneously used the angular diameter distance (D_θ). It has become clear that the correct distance to use in these calculations is the luminosity distance (D_L; see also Sevilla et al. 2026) because the parameter estimation ultimately depends on luminosities (i.e. no angular extent is being directly measured). In the case of AT2023fhn at $z = 0.24$, $D_\theta = 780$ Mpc and $D_L = 1200$ Mpc (for a flat Λ cold dark matter cosmology with $\Omega_m = 0.3$ and $\Omega_\Lambda = 0.7$). We provide updated versions of Table 7 and Figs. 10 and 11 of the original paper in Table 2 and Figs. 3 and 4, where D_L has been used instead. The derived parameter values do not change so much that our conclusions are affected, but we note that making the same error at higher redshifts would be more consequential.

Table 1. Updated unabsorbed X-ray fluxes from the *Chandra* observations of AT 2023fhn (programme 24500143).

Epoch	Start date JD-2460045	$t_{\rm exp}$ ks	F_X erg s^{-1} cm^{-2}
1	14.78957	29.68	$(2.1\pm1.9)\times10^{-14}$
2	27.98310	59.35	$(2.9\pm1.9)\times10^{-15}$
3	61.80356	83.38	$(2.1\pm1.5)\times10^{-15}$
4	198.6632	192.68	$<1.06\times10^{-15}$

Notes. Exposure start times (since JD-2460045), total exposure times, and fluxes are listed. All observations are made with ACIS-S. The fluxes (F_X) are unabsorbed and measured in the energy range 0.5–10.0 keV. Uncertainties are given at 1σ, upper limits at 2σ.

⋆ Corresponding author: ashley.chrimes@esa.int
⋆⋆ ESA research fellow.

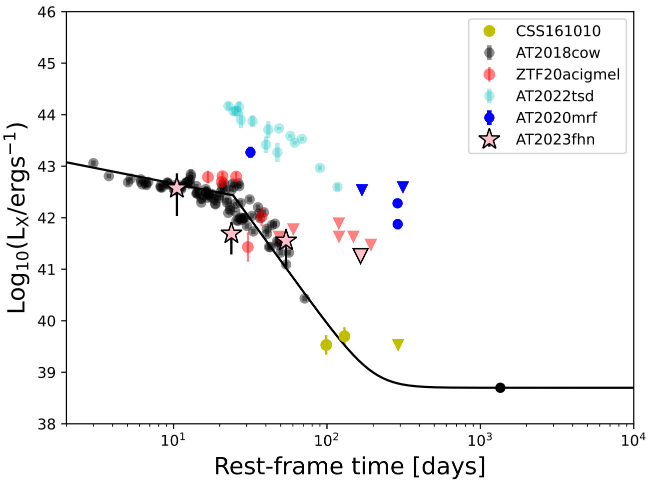

Fig. 1. Update to Fig. 7 of the original paper with the new X-ray measurements for AT2023fhn.

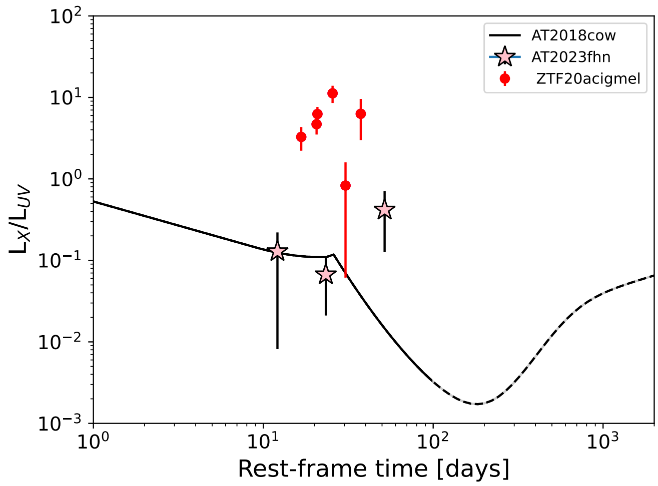

Fig. 2. Update to Fig. 8 of the original paper with the new X-ray measurements for AT2023fhn.

Table 2. Update to Table 7 of the original paper using D_L for the parameter calculations rather than D_θ.

	$t \sim 90$ days	
Parameter	Unit	Value
R_p	10^{17} cm	2.00±0.09
$\Gamma\beta$	–	1.09±0.05
$\dot{M}/v_w$	10^{-4} $M_\odot$ yr^{-1}/1000 km s^{-1}	0.06±0.01
n_e	cm^{-3}	7±0.8
B	G	0.22±0.02
U	10^{49} erg	6.3±0.7
R_p	10^{17} cm	1.78±0.08
$\Gamma\beta$	–	0.97±0.05
$\dot{M}/v_w$	10^{-4} $M_\odot$ yr^{-1}/1000 km s^{-1}	0.78±0.02
n_e	cm^{-3}	(1.1±0.1)×10^2
B	G	0.13±0.01
U	10^{49} erg	55±7
	$t \sim 138$ days	
Parameter	Unit	Value
R_p	10^{17} cm	1.8±0.1
$\Gamma\beta$	–	0.64±0.05
$\dot{M}/v_w$	10^{-4} $M_\odot$ yr^{-1} / 1000 km s^{-1}	0.27±0.08
n_e	cm^{-3}	36±6
B	G	0.29±0.05
U	10^{49} erg	8±2
R_p	10^{17} cm	1.6±0.1
$\Gamma\beta$	–	0.56±0.04
$\dot{M}/v_w$	10^{-4} $M_\odot$ yr^{-1} / 1000 km s^{-1}	3.3±0.1
n_e	cm^{-3}	(5.8±1.0)×10^2
B	G	0.18±0.03
U	10^{49} erg	70±10

Notes. Results above the double horizontal lines assume equipartition ($\epsilon_e = \epsilon_B = 0.33$), and those below assume $\epsilon_e = 0.1$ and $\epsilon_B = 0.01$. Only the equipartition results are plotted in the relevant figures.

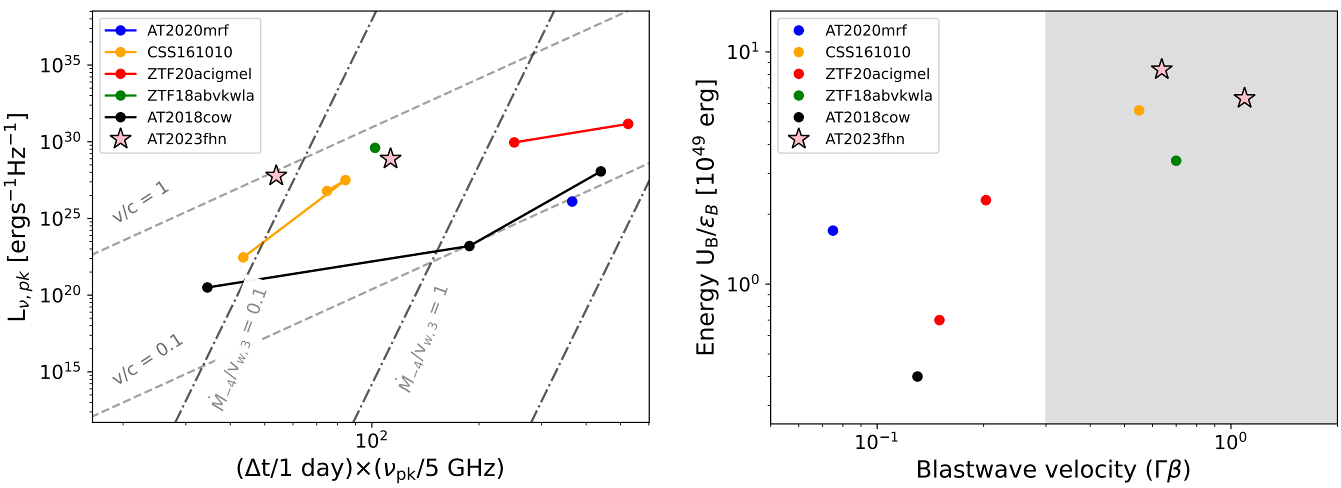

Fig. 3. Update to Fig. 10 of the original paper using D_L rather than D_θ for the parameter estimation of AT2023fhn.

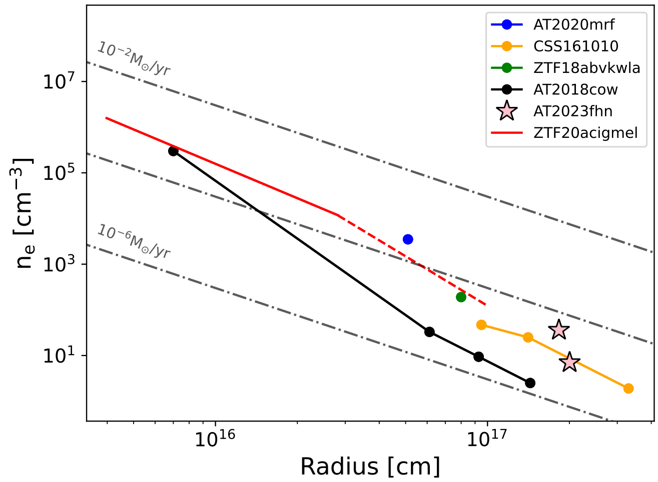

Fig. 4. Update to Fig. 10 of the original paper using D_L rather than D_θ for the parameter estimation of AT2023fhn.

Acknowledgements. The authors thank Raffaella Margutti and Ben Margalit for bringing these points to our attention.

References

Chevalier, R. A. 1998, ApJ, 499, 810
DeMarchi, L., Margutti, R., Dittman, J., et al. 2022, ApJ, 938, 84
Kuin, N. P. M., Wu, K., Oates, S., et al. 2019, MNRAS, 487, 2505
Nayana, A. J., Margutti, R., Wiston, E., et al. 2025, ApJ, 993, L6
Sevilla, C., Ho, A. Y. Q., Nayana, A. J., et al. 2026, ArXiv e-prints [arXiv:2601.18926]
Siemiginowska, A., Burke, D., Günther, H. M., et al. 2024, ApJS, 274, 43